X-591-72-499
PREPRINT

THE BMW ANALYTIC AERODYNAMIC DRAG METHOD FOR THE VINTI SATELLITE THEORY

J. S. WATSON
G. D. MISTRETTA
N. L. BONAVITO

DECEMBER 1972

GODDARD SPACE FLIGHT CENTER
GREENBELT, MARYLAND

THE BMW ANALYTIC AERODYNAMIC DRAG METHOD FOR THE VINTI SATELLITE THEORY

J. S. Watson

G. D. Mistretta

N. L. Bonavito

December 1972

GODDARD SPACE FLIGHT CENTER

Greenbelt, Maryland

CONTENTS

THE BMW ANALYTIC AERODYNAMIC DRAG METHOD FOR THE VINTI SATELLITE THEORY

J. S. Watson

G. D. Mistretta

N. L. Bonavito

ABSTRACT

In order to retain separability in the Vinti theory of earth satellite motion when a non-conservative force such as air drag is considered, a set of variational equations for the orbital elements are introduced, and expressed as functions of the transverse, radial, and normal components of the non-conservative forces acting on the system. In this approach, the Hamiltonian is preserved in form, and remains the total energy, but the initial or boundary conditions and hence the Jacobi constants of the motion advance with time through the variational equations. In particular, the atmospheric density profile is written as a 'fitted' exponential function of the eccentric anomaly, which reproduces tabular values of static model atmospheric densities at all altitudes to within ninety-eight percent and simultaneously reduces the variational equations to indefinite integrals with closed form evaluations, whose limits are in terms of the eccentric anomaly. The values of the limits for any arbitrary time interval are obtained from the Vinti program.

Results of the BMW (Bonavito, Mistretta, Watson) theory for the case of the intense air drag satellites San Marco-2 and Air Force Cannonball are given.

These results indicate that the satellite ephemerides produced by the BMW theory in conjunction with the Vinti program are of very high accuracy. In addition, since the program is entirely analytic, several months of ephemerides can be obtained within a few seconds of computer time.

THE BMW ANALYTIC AERODYNAMIC DRAG METHOD FOR THE VINTI SATELLITE THEORY

INTRODUCTION

In this paper we shall treat the variation of Izsak elements caused by disturbing forces acting on an orbit. These elements, an intrinsic part of the Vinti theory, are obtained as functions of time and then by a process of re-initialization, the Vinti equations of motion are solved for the position and velocity of the satellite. We should note that the air resistance of a body has in general six components, three being forces and three being moments of forces, which tend to make the motion of an asymmetric body very complex. However, for the case of a non-rotating sphere, the resistance can be reduced to a single component directed oppositely to the velocity of the sphere. In this treatment we shall introduce semi-empirically determined components of drag force which are functions of the eccentric anomaly. With use of these, the differential equations for the variation with time of the Izsak elements can be solved along with the Vinti equations of motion.

I. DRAG VARIATIONAL EQUATIONS

Here we present equations for the time rate of change of the Izsak orbital elements of the Vinti satellite theory (Reference 1). In our treatment, we shall assume

that these equations represent instantaneous departures due to aerodynamic drag or perturbing forces on a Vinti orbit. These departures in the Vinti-Izsak orbital elements are then integrated as functions of eccentric anomaly for the instant of time under consideration.

The differential equations representing variations of orbital elements are:

$$\frac{da}{dt} = \frac{2}{na}\frac{\partial \bar{U}}{\partial M}$$

$$\frac{de}{dt} = \frac{1-e^2}{na^2 e}\frac{\partial \bar{U}}{\partial M} - \frac{\sqrt{1-e^2}}{na^2 e}\frac{\partial \bar{U}}{\partial \omega}$$

$$\frac{d\omega}{dt} = \frac{-\cos i}{na^2\sqrt{1-e^2}\sin i}\left(\frac{\partial \bar{U}}{\partial i}\right) + \frac{\sqrt{1-e^2}}{na^2 e}\left(\frac{\partial \bar{U}}{\partial e}\right)$$

$$\frac{di}{dt} = \frac{\cos i}{na^2\sqrt{1-e^2}\sin i}\left(\frac{\partial \bar{U}}{\partial \omega}\right)$$

$$\frac{d\Omega}{dt} = \frac{1}{na^2\sqrt{1-e^2}\sin i}\left(\frac{\partial \bar{U}}{\partial i}\right)$$

$$\frac{dM}{dt} = n - \frac{1-e^2}{na^2 e}\left(\frac{\partial \bar{U}}{\partial e}\right) - \frac{2}{na}\frac{\partial \bar{U}}{\partial a} \qquad (1)$$

where n is related to a by $n^2 a^3 = GM_E = \mu$. G is the gravitational constant, and M_E is the mass of the Earth. Any perturbing force F can be represented

instantaneously as a potential gradient. Let $\bar{U}$ be that potential. We now resolve the perturbing force F into the following components:

R, in the direction of the position vector from the force center to the satellite.

T, is the perpendicular to R, lies in the orbital plane, and is positive in the direction of motion.

W, is mutually perpendicular to R and T and completes a right handed set of component directions.

The partial derivatives appearing in equations (1) are given by:

$$\frac{\partial \bar{U}}{\partial a} = R\left(\frac{r}{a}\right)$$

$$\frac{\partial \bar{U}}{\partial e} = -R\,a\cos v + T\left(\frac{2+e\cos v}{1-e^2}\right) r\sin v$$

$$\frac{\partial \bar{U}}{\partial a} = r\,W\sin\psi$$

$$\frac{\partial \bar{U}}{\partial \Omega} = T\,r\cos i - W(r\cos\psi\sin i)$$

$$\frac{\partial \bar{U}}{\partial \omega} = r\,T$$

$$\frac{\partial \bar{U}}{\partial M} = R\left(\frac{a\,e}{\sqrt{1-e^2}}\right)\sin v + T\left(\frac{a^2\sqrt{1-e^2}}{r}\right) \qquad (2)$$

where ψ is the argument of latitude. Substituting (2) into (1),

$$\frac{da}{dt} = 2\left(\frac{a^3}{\mu}\right)^{1/2} \frac{1}{\sqrt{1-e^2}} \left[Re \sin v + T(1 + e\cos v)\right]$$

$$\frac{de}{dt} = \left(\frac{a}{\mu}\right)^{1/2} \sqrt{1-e^2}\left[R \sin v + T(\cos v + \cos E)\right]$$

$$\frac{di}{dt} = W\left(\frac{r\cos\psi}{na^2\sqrt{1-e^2}}\right)$$

$$\frac{d\omega}{dt} = -R\left(\frac{\sqrt{1-e^2}\cos v}{nae}\right) + T\left(\frac{\sqrt{1-e^2}\left(1+\frac{r}{p}\right)\sin v}{nae}\right) - W\left(\frac{r\cos i \sin\psi}{na^2\sqrt{1-e^2}\sin i}\right)$$

$$\frac{d\Omega}{dt} = W\left(\frac{r\sin\psi}{na^2\sqrt{1-e^2}\sin i}\right)$$

$$\frac{dM}{dt} = n + R\left(\frac{(1-e^2)}{nae}\cos v - \frac{2r}{na^2}\right) - T\left(\frac{(1-e^2)\left(1+\frac{r}{p}\right)\sin v}{nae}\right). \qquad (3)$$

The Vinti parameter related to the orbit inclination is

$$S = \sin^2 i \qquad (4)$$

From this, we have

$$\frac{dS}{dt} = 2\sin i \cos i \frac{di}{dt},$$

or,

$$\frac{dS}{dt} = 2\sqrt{S}\sqrt{1-S}\frac{di}{dt} \quad (5)$$

The variation of the inclination can then be written as

$$\frac{dS}{dt} = \frac{2\sqrt{S(1-S)}\ r W \cos\psi}{\sqrt{\mu a}\sqrt{1-e^2}} \quad (6)$$

Let $\Omega = \beta_3$, $\omega = \beta_2$, and using

$$p = a(1-e^2),$$

$$n^2 a^3 = \mu,$$

$$\sin i = \sqrt{S},$$

we have,

$$\frac{d\beta_2}{dt} = -\left\{\frac{\sqrt{S}\left[aR(1-e^2)\cos v - r(2+e\cos v)T\sin v\right] + r W e \sin\psi\sqrt{1-S}}{(\mu a)^{1/2} e\sqrt{S}\sqrt{1-e^2}}\right\}$$

and

$$\frac{d\beta_3}{dt} = \frac{r W \sin\psi}{(\mu a)^{1/2}\sqrt{S}\sqrt{1-e^2}} \quad (7)$$

The mean anomaly is related to the time of perigee passage β_1 by the expression,

$$M = n(t + \beta_1) \quad (8)$$

From this,

$$\frac{dM}{dt} = \frac{dn}{dt}(t + \beta_1) + n\frac{d\beta_1}{dt} + n$$

or,

$$\frac{d\beta_1}{dt} = \frac{1}{n}\left[\frac{dM}{dt} - (t + \beta_1)\frac{dn}{dt} - n\right] \quad (9)$$

and

$$\frac{dn}{dt} = -\frac{3}{2}\mu^{1/2}a^{-5/2}\frac{da}{dt} \quad (10)$$

together with dM/dt from (3), we find

$$\frac{d\beta_1}{dt} = -\frac{3}{2}\beta_1 a^{-1}\frac{da}{dt} + \mu(-2\alpha_1)^{-3/2}\left\{\frac{3}{2}t\mu^{1/2}a^{-5/2}\frac{da}{dt} - \frac{2r\,R}{(\mu a)^{1/2}} + \frac{(1-e^2)}{e}\left(\frac{a}{\mu}\right)^{1/2}\left[R\cos v - T\left(1 + \frac{r}{a(1-e^2)}\right)\right]\right\} . \quad (11)$$

Summarizing our equations for the time rate of change of orbital elements, we have:

$$\frac{da}{dt} = 2\left(\frac{a^3}{\mu}\right)^{1/2}\frac{1}{\sqrt{1-e^2}}\left[Re\sin v + T(1 + e\cos v)\right]$$

$$\frac{de}{dt} = \left(\frac{a}{\mu}\right)^{1/2} \sqrt{1-e^2}\left[R\sin v + T(\cos v + \cos E)\right]$$

$$\frac{dS}{dt} = \frac{2\sqrt{S(1-S)}\, rW\cos\phi}{(\mu a)^{1/2}\sqrt{1-e^2}}$$

$$\frac{d\beta_3}{dt} = -\frac{rW\sin\phi}{(\mu a)^{1/2}\sqrt{S}\sqrt{1-e^2}}$$

$$\frac{d\beta_2}{dt} = -\left\{\frac{\sqrt{S}\left[aR(1-e^2)\cos v - r(2+e\cos v)T\sin v\right] + reW\sin\phi\sqrt{1-S}}{(\mu a)^{1/2}\sqrt{S}\, e\sqrt{1-e^2}}\right\}$$

$$\frac{d\beta_1}{dt} = -\frac{3}{2}\beta_1 a^{-1}\frac{da}{dt} + n\left(-2\beta_1\right)^{-3/2}\left\{\frac{3}{2}\left(\mu^{1/2}a^{-5/2}\frac{da}{dt} - \frac{2rR}{(\mu a)^{1/2}}\right.\right.$$

$$\left.\left. + \frac{(1-e^2)}{e}\left(\frac{a}{\mu}\right)^{1/2}\left[R\cos v - T\left(1+\frac{r}{a(1-e^2)}\right)\right]\right\}. \qquad (12)$$

Let us now substitute for R, T, and W in terms of the eccentric anomaly as given in reference 2, page 165:

$$R = -\frac{1}{2}C_D\frac{A}{m}ae\rho V\sin E\frac{dE}{dt}$$

$$T = -\frac{1}{2}C_D\frac{A}{m}(1-e^2)^{1/2}a\rho V\left[1-d\,\frac{(1-e\cos E)^2}{(1-e^2)}\right]\frac{dE}{dt} \qquad (13)$$

$$W = -\frac{1}{2} C_D \frac{A}{m} \rho \omega_s V^{-1/2} a^{3/2} \cdot (1 - e\cos E)^2 \sqrt{s} \cos i \frac{dE}{dt}$$

where V is the velocity of the satellite defined by the equation

$$V = \left(\frac{\mu}{a}\right)^{1/2} (1 + e\cos E)^{-1/2} (1 - e\cos E)^{-1/2} \left[(1 + e\cos E) - d(1 + e\cos E)\right] \quad (14)$$

where

$$d = \omega_s \rho^{-1/2} a^{3/2} (1 - e^2)^{1/2} (1 - S)^{1/2} \quad (15)$$

where

ω_s = angular velocity of rotation of earth

ρ = atmospheric density

A = projected area of satellite

m = mass of satellite

C_D = drag parameter (usually around 2.2)

$$\cos v = \frac{\cos E - e}{1 - e\cos E}$$

$$\sin v = \frac{(1-e^2)^{1/2}\sin E}{1-e\cos E} \tag{16}$$

Since the coordinate $\eta = (P + Q\sin\psi)^{-1}\sin i$, and the quantity $\cdot$ of the Vinti potential is approximately 7 kilometers, we then assume $r \cong \rho = a(1 - e\cos E)$, where ρ is an oblate spheroidal coordinate. Now substituting equations (14) and (15) into equations (13), and inserting these results with equations (16) into equations (12), we get

$$\frac{da}{dt} = -C_D\frac{A}{m}\rho a^2\left\{(1-e\cos E)^{-1/2}(1+e\cos E)^{-1/2}\left[(1+e\cos E)\right.\right.$$

$$\left.\left. - d(1-e\cos E)\right]^2\right\}\frac{dE}{dt}$$

$$\frac{de}{dt} = -\frac{1}{2}C_D\frac{A}{m}\rho a(1-e^2)\left\{\left[(1+e\cos E)^{-1/2}(1-e\cos E)^{-3/2}\left[(1+e\cos E)\right.\right.\right.$$

$$\left. - d(1-e\cos E)\right]\left.\right] + \left[e\sin^2 E + (1-e^2)^{-1}\left[(1-e^2)\right.\right.$$

$$\left.\left.\left. - d(1-e\cos E)^2\right]\left[(\cos E - e) + \cos E(1-e\cos E)\right]\right]\right\}\frac{dE}{dt}$$

$$\frac{dS}{dt} = -C_D \frac{A}{m} \sqrt{S(1-S)}\, \rho^{-1/2} a^{5/2} (1-e^2)^{-1/2}$$

$$\cdot \left\{ \cos^2 \phi (1 - e\cos E)^{3/2} (1 + e\cos E)^{-1/2} \left[(1 + e\cos E) - d(1 - e\cos E) \right] \right\} \frac{dE}{dt}$$

$$\frac{di_2}{dt} = -\frac{1}{2} C_D \frac{A}{m} \sqrt{ae^{-1}} (1-e^2)^{-1/2} \left\{ e \sin\phi \cos\phi (1-S)^{1/2} \sqrt{\mu}^{-3/2} a^{3/2} \right.$$

$$\cdot (1 + e\cos E)^{-1/2} (1 - e\cos E)^{5/2} \left[(1 + e\cos E) \right.$$

$$\left. - d(1 - e\cos E) \right] \cdot (1 - e\cos E)^{-3/2} (1 + e\cos E)^{-1/2} \left[(1 + e\cos E) \right.$$

$$\left. - d(1 - e\cos E) \right] \left[2\sin E(1-d) + de^2 \sin E(1 + e^2\cos^2 E) + de \sin E \cos E \right.$$

$$\left. - 4e^2 \sin E(1 - d\cos^2 E) + 2e^4 \sin E(5 - 2e^2 + e^2\cos^2 E) \right] \left. \right\} \frac{dE}{dt}$$

$$\frac{di_3}{dt} = \frac{1}{2} C_D \frac{A}{m} \sqrt{\rho_s} \sqrt{\mu}^{-1/2} a^{5/2} (1-e^2)^{-1/2}$$

$$\times \left\{ \sin\phi \cos\phi (1 - e\cos E)^{5/2} (1 + e\cos E)^{-1/2} \left[(1 + e\cos E) \right. \right.$$

$$\left. \left. - d(1 - e\cos E) \right] \right\} \frac{dE}{dt}$$

$$\frac{d\sigma_1}{dt} = -\mu(-2t_1)^{-3/2}\left\{\frac{3}{2}(t_0-t_1)^{1/2}a^{-5/2}\frac{da}{dt}\right.$$

$$+(1-e^2)^{1/2}\left[\frac{d\sigma_2}{dt}-\sqrt{1-S}\,\frac{d\sigma_3}{dt}\right]$$

$$+C_D\frac{A}{m}\rho ae\left[\sin E(1-e\cos E)^{1/2}(1+e\cos E)^{-1/2}\left[(1+e\cos E)\right.\right.$$

$$\left.\left.-d(1-e\cos E)\right]\right]\frac{dE}{dt}\Bigg\}-\frac{3}{2}\frac{1}{a}(t_0-t_1)\frac{da}{dt}\,. \qquad (17)$$

If we indicate the eccentric anomaly at time t_1 by E_1 and at time t_2 by E_2, the solutions of equations (17) are given by the following:

$$\Delta a = -C_D\frac{A}{m}a^2\int_{E_1}^{E_2}\rho(1-e\cos E)^{-1/2}(1+e\cos E)^{-1/2}\left[(1+e\cos E)\right.$$

$$\left.-d(1-e\cos E)\right]^2\Big\}\,dE$$

$$\Delta e = -\frac{1}{2}C_D\frac{A}{m}(1-e^2)a\int_{E_1}^{E_2}\rho\left\{\left[(1+e\cos E)^{-1/2}(1-e\cos E)^{-3/2}\left[(1-e\cos E)\right.\right.\right.$$

$$\left.-d(1-e\cos E)\right]\left[e\sin^2 E+(1-e^2)^{-1}\left[(1-e^2)\right.\right.$$

$$\left.\left.\left.-d(1-e\cos E)^2\right]\left[(\cos E-e)+\cos E(1-e\cos E)\right]\right]\right\}dE$$

$$\Delta S = -C_D \frac{A}{m} \rho_s S \sqrt{1 - S}\, a^{-1/2} a^{5/2} (1 - e^2)^{-1/2}$$

$$\times \int_{E_1}^{E_2} \cos\gamma \,(1 - \cos E)^{5/2} (1 + e\cos E)^{-1/2} \,[(1 + e\cos E)\, d(1 - e\cos E)]\, dE$$

$$\Delta\beta_2 = -\frac{1}{2} C_D \frac{A}{m} a e^{-1} (1 - e^2)^{-1/2} \int_{E_1}^{E_2} \rho_s e \sin\gamma \cos\gamma \,(1 - S)^{1/2} \rho_s a^{-3/2} a^{3/2}$$

$$\times (1 + e\cos E)^{-1/2} (1 - e\cos E)^{5/2} [(1 + e\cos E)$$

$$- d(1 - e\cos E)] + (1 - e\cos E)^{-3/2} (1 + e\cos E)^{-1/2} [(1 + e\cos E)$$

$$- d(1 - e\cos E)] [2\sin E (1 - d) - 4e^2 \sin E (1 + d\cos^2 E) + 2e^4 \sin E$$

$$+ d e^2 \sin E (1 + e^2 \cos^2 E) + de \sin E \cos E (5 - 2e^2 + e^2 \cos^2 E)]\} dE$$

$$\Delta\beta_3 = -\frac{1}{2} C_D \frac{A}{m} \rho_s a^{-1/2} a^{5/2} (1 - e^2)^{-1/2}$$

$$\times \int_{E_1}^{E_2} \sin\gamma \cos\gamma \,(1 - e\cos E)^{5/2} (1 + e\cos E)^{-1/2} [(1 + e\cos E)$$

$$- d(1 - e\cos E)]\, dE$$

$$[illegible] \left\{ \frac{3}{2} [illegible] \right.$$

$$+ (1 - e^2)^{1/2} [illegible]$$

$$+ [illegible] \frac{A}{m} [illegible] \int_{E_1}^{E_2} \sin E \, (1 [illegible] e \cos E)^{1/2} (1 [illegible] e \cos E)^{-1/2} (1 [illegible] e \cos E)$$

$$\left. - d(1 - e \cos E)] \, dE \right\} - \frac{3}{2} \, \frac{1}{a} (t_0 - [illegible]) [illegible] \quad (18)$$

II. ATMOSPHERIC DENSITY REPRESENTATION

At this point we consider the expression for atmospheric density variation given by King-Hele (Reference 3). An expression for the atmospheric density as a function of the eccentric anomaly is given by

$$\rho = \rho_p \{1 + b(r - r_p)^2\} \exp \left(- \frac{r - r_p}{H_p} \right)$$

$$= \rho_p \{1 + bx^2 (1 - \cos E)^2\} \exp \left\{ - \frac{x}{H_p} (1 - \cos E) \right\} \quad (1)$$

where $x = ae$, H_p = density scale height at perigee which in equation (1) is assumed to vary linearly with the perigee height.

Let us now write equation (1) in a more general form so as to represent the atmospheric density variation over any interval within the orbit in which the boundary conditions are known. A generalization of (1) is desirable for

our purposes to insure that the resultant analytic atmospheric model rigidly adheres to a tabular set of densities at all altitudes. To obtain this generalization, let the subscripts L and U refer to a lower and upper point of an interval respectively. This interval $[E_L, E_U]$ is judiciously chosen (by a method discussed later in this section) to allow ρ to be given by an expression of the type of equation (1), over this restricted domain $[E_L, E_U]$. Let,

$$\rho(r) = \rho_L \left\{1 + b(L, U)\,(r - r_L)^2 \exp\left(-\frac{r - r_L}{H_L}\right)\right\}, \quad r_L \le r \le r_U$$

$$= \rho_L \left\{1 + b(L, U)\, x^2 (\cos E_L - \cos E)^2\right\} \exp\left\{-\frac{x}{H_L}(\cos E_L - \cos E)\right\}, \quad E_L \le E \le E_U \tag{1.1}$$

where ρ_L and H_L are available from density tables, E_L and E_U are available from the orbit theory (as are r_L and r_U), and b(L, U) is derivable from (1.1) by setting $\rho = \rho_L$ and forming the inverse transformation

$$b(L, U) = b(L, U; \rho_L, \rho_U, r_L, r_U, H_L). \tag{1.2}$$

If equation (1.1) above is substituted into (I-18), the resulting expressions for the variational equations reduce to the form

$$\int_{E_1^*}^{E_2^*} \sin^n E \cos^m E \exp\{-(x/H_L)(\cos E_L - \cos E)\}\, dE \tag{2}$$

where H_L is held constant over the range of a subinterval of integration and x is held constant over the entire range of integration. Since however, the parameter n can assume the value zero, we are forced to alter the form of (2) so as to insure that the expression under the integral sign is integrable while simultaneously maintaining its theoretical physical content. In short, the variational equations cannot be evaluated by the Fundamental Theorem of Calculus since an antiderivative of $\sin^n E \cos^m E \exp\{-(x/H_L)(\cos E_L - \cos E)\}$ is not expressible in terms of elementary functions.

To achieve this purpose, let us now consider the following:
Rewrite the expression for atmospheric density (1) in the form

$$\rho_L [1 + b(L, U) x^2 (\cos E_L - \cos E)^2] b_1(E) \exp [b_2(E) \cdot E]$$

$$E_L \leq E \leq E_U \qquad (3)$$

where $b_1(E)$, $b_2(E)$ are arbitrary functions of E which will be chosen to preserve closed form integrability of the variational equations (I-18) while retaining near complete numerical agreement with the exponential term of the King-Hele's expression for ρ (E).

The selection of the two functions $b_1(E)$, $b_2(E)$ between an upper limit of integration E_2 and a lower limit E_1 will be made in the following manner. Consider the interval $[E_1^*, E_2^*]$ subdivided into a collection of n nonoverlapping subintervals I_i, ($i = 1, 2, \ldots, n$), defined by the partitioning

$$E_1^* = x_0 < x_1 < \cdots < x_{n-1} < x_n = E_2^*.$$

For any subinterval $I_i = [x_{i-1}, x_i)$, define

$$\begin{aligned} b_1(E) &= c_i \quad \text{for} \quad x_{i-1} \le E < x_i \\ b_2(E) &= d_i \end{aligned} \tag{4}$$

where c_i, d_i are constants. The determination of c_i, d_i will be accomplished by applying the technique of classical weighted least squares. In this manner the definition of $b_1(E)$ and $b_2(E)$ over the domain $[E_1^*, E_2^*]$ are the step functions

$$\begin{aligned} b_1(E) &= c_1 \quad x_0 \le E < x_1 \\ &= c_2 \quad x_1 \le E < x_2 \\ &\vdots \qquad \vdots \\ &= c_n \quad x_{n-1} \le E \le x_n \end{aligned} \tag{5}$$

$$\begin{aligned} b_2(E) &= d_1 \quad x_0 \le E < x_1 \\ &= d_2 \quad x_1 \le E < x_1 \\ &\vdots \qquad \vdots \\ &= d_n \quad x_{n-1} \le E \le x_n. \end{aligned}$$

Consider observational data Y_i generated with I_L by repeated evaluation of the function

$$h(E_i) = \exp\left[-\alpha(\cos E_i - \cos E_t)\right]$$

where $\alpha = x/H_L$ and $x_{t-1} \leq E_i \leq x_t$. To define the pseudo-regression situation governing our estimation problem, consider the implicitly linear, exponential model

$$Y_i = \beta_1 \epsilon_i \exp(\beta_2 E_i) \qquad i = 1, 2, \cdots, m \tag{6}$$

relating the concomitant variable E and the dependent or response variable Y that, unlike the general regression response variable, displays no random variability. Hence, the random variables ϵ_i denoting the dispersion characteristics of Y_i about the theoretical regression line become meaningless in the curve fitting analysis. That is, the random variables ϵ_i are degenerate in the sense that their probability density functions $p(\epsilon_i)$ are given by

$$\begin{aligned} p(\epsilon_i) &= 1 \qquad \epsilon_i = B_i \\ &= 0 \qquad \text{otherwise} \end{aligned} \tag{7}$$

where B_i can be considered a "fitting bias" at $E = E_i$ since

$$E(\epsilon_i) = B_i \qquad \text{Var}(\epsilon_i) = 0. \tag{8}$$

While all practical statistical properties of the regression analysis become lost, the technique is not degraded as a numerical tool for approximating with great precision complex functional forms over restricted regions with relatively simple functions.

To display the implicit linear form of (6), we take the natural logarithm of both sides of (6) and obtain the equivalent form

$$\ln Y_i = \ln \beta_1 + \beta_2 E_i + \ln \varepsilon_i$$

or

$$Y_i' = \beta_1' + \beta_2 E_i + \varepsilon_i' \quad (i = 1, 2, \cdots, m) \tag{9}$$

If nonnegative weights $\omega_1, \omega_2, \ldots, \omega_m$ are available and the y_i' are evaluated from $y_i' = \ln h(E_i) = -\tfrac{1}{2}(\cos x_{j-1} - \cos E_i)$, then the well known result

$$b_1' = \left(\sum_1^m \omega_i\right)^{-1} \sum_1^m \omega_i y_i' - b_2 \left(\sum_1^m \omega_i\right)^{-1} \sum_1^m \omega_i E_i$$

$$b_2 = \frac{\sum_1^m \omega_i y_i' E_i - \left(\sum_1^m \omega_i\right)^{-1} \left(\sum_1^m \omega_i y_i'\right)\left(\sum_1^m \omega_i E_i\right)}{\sum_1^m \omega_i E_i^2 - \left(\sum_1^m \omega_i\right)^{-1} \left(\sum_1^m \omega_i E_i\right)^2} \tag{10}$$

are the values of β_1', β_2 that minimize the weighted sum of squares

$$\sum_1^m \omega_i \varepsilon_i'^2 = \sum_1^m \omega_i (y_i' - \beta_1' - \beta_2 E_i)^2. \tag{11}$$

Thus, $b_1 = \exp(b_1')$ and b_2 are the classical weighted least squares estimates of β_1, β_2 respectively.

The selection of the mesh points over an interval of integration $[E_1^*, E_2^*]$ is obtained through an automated search approach utilizing the constrained weighted least squares process previously described. This technique selects subintervals of maximum size while retaining a user selected error tolerance between the true and predicted function.

Furthermore, if one sets $E_1^* = 0$, $E_2^* = \pi$, and derives a set of coefficients for the n selected subintervals in the manner previously defined, the functions h(E) and . (E) will have been fit for all values of E over which x has been assumed constant. This is true since h(E) is a periodic function with period 2π and in the fundamental period $(0, 2\pi)$ is symmetrically distributed about the axis of symmetry $E = \pi$.

With the use of more general expression for density (e), the variational equations (I-17) integrated between E_1^* and E_2^* where $0 < E_1^* < E_2^* < \pi$, take on the following form:

$$\Delta q_k = \sum_{j=0}^{n-1} \int_{x_j}^{x_{j+1}} \{t_{j+1} \exp(d_{j+1} E)\} dG_k(E) \quad (k = 1, 2, \cdots, 6). \tag{12}$$

Having fit h(E) from $(0 - \pi)$, the integration of the variational equations between any two arbitrary limits $E_1^* \geq 0$, $E_2^* > E_1^*$, takes the general form

$$\begin{aligned}
\Delta q_k = & \sum_{j=0}^{n-1} m_{j+1} \int_{x_j}^{x_{j+1}} \{t_{j+1} \exp[d_{j+1} E]\, dG_k(E) \\
& + \sum_{j=0}^{n-1} m_{2n-j} \int_{2\pi - x_{j+1}}^{2\pi - x_j} \{t'_{2n-j} \exp[d'_{2n-j} E]\} dG_k(E) \\
& + \int_{x_\xi}^{E_2^* \bmod 2\pi} t_\xi^* \exp(d_\xi^* E)\, dG_k(E) \\
& + \int_{E_1^* \bmod 2\pi}^{x_\eta} t_\eta^* \exp(d_\eta^* E)\, dG_k(E) \quad (k = 1, 2, \cdots, 6)
\end{aligned} \tag{13}$$

where m_i, ($i = 1, 2, \ldots, 2n$), are nonnegative integers; t_j, t'_k, d'_k ($j = 1, 2, \ldots, n$), ($k = n+1, n+2, \ldots, 2n$) are functions of c_j, d_j; ξ is an integer between 0 and $2n-2$; η is an integer between 1 and $2n-1$; the grid points x_{n+1}, x_{n+2}, $\ldots$, x_{2n} are defined from $x_0, x_1, \ldots, x_n$; and (t^*_ξ, t^*_η) may be either (t_ξ, t_η), (t'_ξ, t_η), (t_ξ, t'_η), (t'_ξ, t'_η) depending upon the values $E_1^* \bmod 2^{\xi}$, $E_2^* \bmod 2^{\eta}$. The logical structure of (13) and the determination of the above parameters is too lengthy to be given here but is presented in Appendix for completeness. It must be emphasized that (13) is general for all computations, but is valid only while x is assumed constant, whereby a new fit is obtained and new constants are determined to integrate (I-13) by the general form (13).

Using these results we can now solve the density expression for the value of b within each of the selected or fitted intervals from the expression,

$$b(L, U) = \frac{-\rho_L + \rho_U \exp\left[(r_U - r_L)/H_L\right]}{\rho_L (r_U - r_L)^2} \tag{14}$$

where the subscripts U and L still refer to the upper and lower points of an interval. For example, ρ_L is that value of density at the initial point of the interval which is known from the tables, and the corresponding density scale height H_L can then be computed. The end point r_U is known as a function of E. Therefore H_L is also 'advanced' in a similar fashion as ρ_L during the fitting of the exponential. The above method of fitting King-Hele's expression over several intervals of an orbit is sufficient to 'reproduce' the tabular model atmosphere to within

ninety-eight percent at all points, and simultaneously yield closed form integrable equations for the variation of the elements. Table I provides a list of computed versus static model atmosphere densities for various altitudes and the differences, as experienced by the San Marco-2 satellite during a revolution using the Spring-Fall Model with an Exospheric temperature of 1100°K. Where the density is high, as for example the critical region around perigee, the difference between calculated and tabular values are 10^{-2} grams/(km)^3 or less. Since b(L, U) is determined by r_0 to be at the upper end of each arc, then the density differences at this point become vanishingly small.

III. SOLUTION OF VARIATIONAL EQUATIONS

In light of the analysis done in section II above, we now return to the variational equations (I-18). If we now combine the radical terms in (I-18), we obtain a set of expressions containing the forms $(1 \pm \chi)^n$, and $(1 \pm \chi)^{-n}$, where $n = 1/2$ and $\chi = e^2 \cos^2 E$. If one assumes that χ will never get too large, that is, for drag satellites, e will not be larger than 0.2, then the above terms can be expanded as,

$$(1 \pm \chi)^n = 1 \pm n\chi + \frac{n(n-1)}{2}\chi^2.$$

and

$$(1 \pm \chi)^{-n} = 1 \mp n\chi + \frac{n(n+1)}{2}\chi^2. \qquad (1)$$

Adopting expression (II-1.1) for atmospheric density variation, the variational equations are then reduced to solving a set of indefinite integrals of the form

$$k_i \int_{E_1^*}^{E_2^*} \exp -(x\ H_L)\ (\cos E_L - \cos E)^{\ell} \cos^{\ell} E \sin^{p} E\ dE \qquad (2)$$

where k_i is simply the constant coefficient of each corresponding integral. If, on the other hand, the eccentricity is somewhat larger than normal, say around 0.5 or so, then it will be necessary to include several more terms in the expansion (1) above. This however is an algebraic problem, and computationally speaking has only the effect of changing the overall coefficients, k_i, in the final algorithm. The integrals are still of the form (2) above. Utilizing the fitting described in section II, the exponential of the density can now be represented as

$$b_1(E) \exp [b_2(E) \cdot E] \qquad (3)$$

in which $b_1(E)$ and $b_2(E)$ are determined for one or several segments within an orbital revolution. Results indicate that $b_1(E)$ and $b_2(E)$ remain fixed for a considerable length of the satellite's lifetime. Refitting becomes necessary only when a and e change appreciably. This is found to occur more frequently near the end of the satellite's lifetime. In any event, the fitting procedure is instantaneous, and the calculation proceeds without interruption.

Using these results, equation (2) can now be rewritten as

$$\int_{E_1^*}^{E_2^*} b_1(E) \exp [b_2(E)\ L] \cos^{\ell} E \cdot \sin^{p} E\ dE \qquad (4)$$

Here p takes the values 0, 1, and 2. When p = 0, ℓ takes on all values from zero through twelve. When p = 1, ℓ goes from zero through eleven, and where p = 2, ℓ ranges from zero through ten. When p = 0, equation (4) is a recursion solution given by a summation whose terms take the form

$$\frac{\exp\left[b_2(E)\cdot E\right]\cos^{\ell-1}E(b_2\cos E + \ell\sin E)}{b_2^2+\ell^2}\Bigg|_{E_L}^{E_U} + \frac{\ell(\ell-1)}{b_2^2+\ell^2}\int_{E_L}^{E_U}\exp\left[b_2(E)\cdot E\right]\cos^{(\ell-2)}E\,dE. \tag{5}$$

where b_2 is taken constant within the subinterval $[E_L,\ E_U]$ of the interval $[E_1^*,\ E_2^*]$. When p = 1 or 2, the recursion solution summation terms become after some reduction,

$$\frac{-\exp\left[b_2(E)\cdot E\right]\cos^{\ell}E}{\ell}\Bigg|_{E_L}^{E_U} + \frac{b_2}{\ell}\int_{E_L}^{E_U}\exp\left[b_2(E)\cdot E\right]\cos^{\ell}E\,dE. \tag{6}$$

If in the drag acceleration one desires to express the velocity and density exponential so as to involve the product of J_2, the coefficient of the earth's second zonal harmonic, and the air density ρ, one can follow the procedure of Sherrill (Reference 4) and write these terms as,

$$v = \left(\sqrt{\frac{\mu}{a}}\right)\ 2\left[\left(\frac{a}{\rho}\right) - 1\right]^{1/2}$$

$$- 2\,\frac{c^2}{a^2}\left(\sqrt{\frac{\mu}{a}}\right)\frac{(1-\eta_0^2)}{(1-\epsilon^2)}\left(\frac{a}{\rho}\right)^2\left[2\left(\frac{a}{\rho}\right) - 1\right]^{-1/2}\ \frac{\eta_0^2\cos^2\psi}{1-\eta^2}$$

$$+\frac{1}{2}\frac{e^2}{a^2}\left(\sqrt{\frac{\mu}{a}}\right)\frac{(1-e_0^2)}{(1-e^2)}\left[2\left(\frac{a}{r}\right)-1\right]^{-1/2}-\frac{1}{2}\frac{e^2}{a^2}\left(\sqrt{\frac{\mu}{a}}\right)\frac{2}{n_0}\left(\frac{a}{r}\right)^3\left[2\left(\frac{a}{r}\right)-1\right]^{-1/2}$$

$$+\frac{1}{2}\frac{e^2}{a^2}\left(\sqrt{\frac{\mu}{a}}\right)\frac{2}{n_0}\left(\frac{a}{r}\right)^3\left[2\left(\frac{a}{r}\right)-1\right]^{-1/2}\cos 2\phi \qquad (7)$$

and

$$\exp\left\{-(x/H_L)\left[\left(\frac{r}{a}\right)+\frac{1}{2}\frac{e^2}{a^2}\left(\frac{a}{r}\right)(1-\sin^2\phi)\right]\right\}\exp\left[-(x/H_L)\cdot u\right] \qquad (8)$$

where

$$u\left(\frac{r}{a}\right)+\frac{1}{2}\frac{e^2}{a^2}\left(\frac{a}{r}\right)(1-\sin^2\phi),$$

and e^2 is approximated by $e^2 = J_2 R_e^2$, where R_e is the value of the earth's equatorial radius (Reference 1). If e^2 is taken to be zero here, then these cross products in v are ignored and (7) and (8) reduce to those expressions given in Section I. Results from low perigee satellites such as OAR-901 (Cannonball) show that the e^2 terms of equation (7) make differences only in the sixth decimal place in the variational equations. In addition, the cross term in the exponential is 10^3 times those corresponding terms in the velocity. Since this correction is accounted for rather simply by the fitting procedure, the cross term is retained in the exponential.

The solutions of the variational equations are added to the epoch values of the Izsak elements in the Vinti program, thus enabling the program to produce an ephemeris which includes the effect of aerodynamic drag. In effect, the original separability is maintained, and the initial or boundary conditions are advanced using an analytic or closed form solution for the variational equations.

IV. RESULTS

In order to test the BMW theory, two heavy air drag satellites with somewhat dissimilar characteristics are considered. These are the Italian San Marco-2 and the U.S. Air Force Cannonball (OAR-901). Data on these spacecrafts is as follows:

San Marco-2:

Mass m = 129.27383 kgm.

Projected Area A = 3425.3397 cm^2.

Drag Coefficient C_D = 2.1

Initial epoch: April 26, 1967, 10 hours, 12 minutes.

Initial conditions:

$x = +0.58725272, \qquad \dot{x} = -0.82890608$

$y = +0.84923499, \qquad \dot{y} = +0.56396878$

$z = -0.05068537, \qquad \dot{z} = +0.01219124$

Here, x, y, and z are in units of earth radii (6378.166 kilometers), and $\dot{x}$, $\dot{y}$, and $\dot{z}$ in units of earth radii per canonical unit of time (806.812 seconds).

Apogee height = 736.00 kilometers

Perigee height = 205.60 kilometers

Eccentricity = 0.0387

Inclination = 2.87 degrees.

Cannonball:

Mass m = 362.87392 kgm.

Projected Area A = 3423.6195 cm^2.

Drag Coefficient $C_D = 2.1$

Initial Epoch: August 7, 1971, 0 hours, 20 minutes.

Initial Conditions:

$x = -0.9428339$, $\dot{x} = -0.26977565$

$y = -0.28161629$, $\dot{y} = -0.40945775$

$z = +0.28038380$, $\dot{z} = -1.0092100$

Apogee height = 1957.20 kilometers

Perigee height = 130.16 kilometers

Eccentricity = 0.1230

Inclination = 92.00 degrees.

In both cases, the boundary values of the atmospheric density profile given by ρ_L are taken from a static model, namely, the 1966 U. S. Standard Air Force Supplements. The profiles used here include a Spring-Fall model with an 1100 degree exospheric temperature, a Winter, 800 degree model, and a Summer 1000 degree model. While these profiles are adequate if chosen carefully, it is felt that a somewhat more sophisticated and dynamic model such as given by Jacchia (Reference 5) would not only improve results but also make them more reliable.

Figure 1, shows the variation over one orbital period (from time of insertion) of the semi-major axis, eccentricity, and $(\beta_2 + \beta_3)$ respectively for San Marco-2. Here, a_0 and c_0 are taken to be the initial values of these parameters. For the semi major axis, we have initially a secular decrease of

198 parts in 10^6 per revolution, with a periodic variation superimposed, of about 25 parts in 10^6 with the orbital period. The eccentricity shows a secular decrease of approximately 97 parts in 10^6 per revolution, and a periodic variation superimposed on it with an amplitude of about 22×10^{-6}, with the orbital period. Figure 1 shows that ($_2$ + $_3$) shifts back and forth by about 8.3 seconds. Figure 2 is a similar graph for Cannonball. It is seen that the variations for a and e here are somewhat larger than for San Marco-2 while the shift of ($_2$ + $_3$) is considerably less. This behavior is what one would expect considering the differences in the orbits.

Figures 3 and 4 are graphs of semi-major axis versus time (days from insertion), for San Marco-2 and Cannonball during an actual lifetime study for the two satellites. The circles are those values of a, predicted by the BMW theory using only the initial conditions given above, while the crosses indicate those arcs of data supplied by orbit improvement routines utilizing tracking or observational data to update the orbital elements. The orbital improvements were necessitated by the rapid deterioration of the orbital parameter quality due to inaccurate force modeling (particularly air resistance accelerations) in the equations of motion. The accepted date of re-entry into the earth's atmosphere for San Marco-2 was on October 14, 1967 at approximately 13 hours. Thus, the total lifetime was about 171 days. The BMW program computed a lifetime of 165 days, for a re-entry on October 8, 1967. Cannonball's re-entry date was approximately January 28, 1972, a lifetime of about 173 days. BMW computed

170 days. In these two cases, the program evaluated the limits of the variational equations for values of the eccentric anomaly corresponding to five day intervals. This was done so as to allow the BMW program to compare at intermediate points, its values for semi-major axis with the observed ones. In actual practice, these limits would be evaluated for those values of eccentric anomaly corresponding to those regions of an orbit over which a fit of the density variation remained fixed. Using a change in perigee height criterion (preselected at 1 km), results from Cannonball show that the first region is the first 65 days, the second is the next 55 days, and so on, until within the last month of life the regions are only of 5 day durations. As a result, the entire ephemeris is computed rapidly. Using the IBM 360/91 electronic digital computer, the complete San Marco-2 and Cannonball ephemerides computed at 5 day intervals were executed in less than 18 seconds of computer CPU time.

These results show that the BMW program was within 4 percent of the "true" lifetimes of both satellites, despite the fact that Cannonball had a relatively high eccentricity and low perigee. In addition, it must be pointed out that the initial conditions used in the program were obtained from orbit improvement routines other than the Vinti Orbit Determination System (References 6, 7), since this was the only data available. To be more consistent, and to improve accuracy, one should utilize, if possible, only those initial or epoch values obtained from the Vinti Orbit Determination System.

In spite of the startling success with San Marco-2 and Cannonball, improvements to the present BMW computer program are being considered. Prime among these is the incorporation of a dynamic model atmospheric density profile such as Jacchia's. As is well known a slight miscalculation in the exospheric temperature for a static model would drastically alter the resulting density profile, and consequently, the computed ephemeris of the satellite.

The distinct advantage of the BMW method over numerical integration techniques is that being analytic or closed form, it is not subject to large error accumulation due to roundoff and truncation. In addition, an entire ephemeris can be obtained in a matter of a few seconds on present generation computers, while such a task might be prohibitive with a numerical integration.

With the atmospheric approximation of this paper, equation (III-3) could be expressed in terms of Bessel functions, for example,

$$\frac{1}{\pi}\int_0^{\pi} \exp(c\cos E)\cos^n E\,dE = I_0(c) \qquad (n = 0)$$

$$= I_1(c) \qquad (n = 1)$$

$$= I_0(c) - \frac{1}{c} I_1(c) \qquad (n = 2)$$

and so forth. The disadvantage here, besides the limited step size over which to perform the summation, is in the difficulty of handling intermediate points

within the limits. A Bessel function approach would appear to be better employed in a study of atmospheric density inference from calculations of the period decrement.

King-Hele (Reference 3) has studied the contraction of orbits in a closed form manner. Four situations are considered:

1. Normal e, Phase 1: approx. $0.02 < e < 0.2$ ($3 < (ae/H_p) < 30$ approx.)
2. Normal e, Phase 2: $0 < e < 0.02$ approx. ($0 < (ae/H_p) < 3$)
3. Circular orbits: $e = 0$ ($ae/H_p = 0$).
4. High eccentricity: $e \geq 0.2$ ($ae/H_p \geq 30$ approx.).

It is felt that the regions covered by the equations of motion in these four cases are also covered by the BMW theory. Even though a static model atmosphere profile was used in the calculations, BMW does have the latitude of utilizing a density profile such as the Jacchia model. In addition, the reference orbit is not an exact ellipse, but the Vinti orbit. As a result, it is felt that the BMW method has contributed to the program for calculating both accurately and rapidly, the orbits of satellites experiencing aerodynamic drag.

At the present time, the Vinti differential correction algorithm (Reference 7) employing a classical weighted least squares technique is being appropriately modified to accommodate the augmented force model. The bulk of the implementation requires the reformulation of the partial derivatives $\{\partial y_i / \partial q_j(t_0)\}$ to reflect air drag where $\{y_i\}$ are tracking observables and $\{q_j(t_0)\}$ are the set of "epoch" Vinti orbital elements and an atmospheric parameter iteratively

estimated by the differential correction technique. It appears that complete analyticity can be retained for these partial derivative expressions, thus merging the theoretical developments presented here with the practical application of orbit estimation. This work will be forthcoming in a future report.

ACKNOWLEDGMENTS

The authors are grateful to Dr. John P. Vinti of the Measurement Systems Laboratory, Massachusetts Institute of Technology, Cambridge, Massachusetts, for valuable discussions which contributed to this report, and to Mr. E. M. Jones of the Goddard Space Flight Center for his assistance with some of the numerical calculations of this report.

REFERENCES

1. Vinti, John P., "Improvement of the Spheroidal Method for Artificial Satellites," Astronomical Journal, 74, Number 1, p. 25-34, February, 1969.

2. Sterne, T. E., "An Introduction to Celestial Mechanics," Interscience Publishers, Inc., New York, 1960.

3. King-Hele, Desmond, "Theory of Satellite Orbits in an Atmosphere," Butterworth and Co. (Publishers) LTD., London, 1964.

4. Sherrill, T. J., "Development of a Satellite Drag Theory Based on the Vinti Formulation," (Ph. D. Dissertation), University of California, Berkley, 1966.

5. Roberts, C. E., "An Analytic Model for Upper Atmosphere Densities based upon Jacchia's 1970 Models," Celestial Mechanics Journal, 4, p. 368-377, 1971.

6. Bonavito, N. L., "Computational Procedure for Vinti's Accurate Reference Orbit with Inclusion of the Third Zonal Harmonic," NASA Technical Note D-3562, August 1966.

7. Walden, H. and Watson, J. S., "Differential Corrections Applied to Vinti's Accurate Reference Satellite Orbit with Inclusion of the Third Zonal Harmonic," NASA Technical Note D-4088, August 1967.

TABLE I

Height	Static ATM Density	RHO	DIFF.
0.205000000000D 03	0.301060802633D 03	0.301060802633D 03	0.0
0.206000000000D 03	0.292581857391D 03	0.292581857391D 03	0.113686837722D-12
0.207000000000D 03	0.284373995477D 03	0.284373956992D 03	0.384845234862D-04
0.208000000000D 03	0.276427541284D 03	0.276427541284D 03	0.113686837722D-12
0.209000000000D 03	0.268733199909D 03	0.268733129768D 03	0.701411933051D-04
0.210000000000D 03	0.261282040805D 03	0.261281906415D 03	0.134389794596D-03
0.211000000000D 03	0.254065482185D 03	0.254065482185D 03	0.213162820728D-13
0.212000000000D 03	0.247075275161D 03	0.247075072937D 03	0.202224049809D-03
0.213000000000D 03	0.240303494560D 03	0.240302827238D 03	0.667321502970D-03
0.214000000000D 03	0.233742515394D 03	0.233741317168D 03	0.119822619084D-02
0.215000000000D 03	0.227385009955D 03	0.227383376171D 03	0.163178351055D-02
0.216000000000D 03	0.221223930490D 03	0.221222099643D 03	0.183084742285D-02
0.217000000000D 03	0.215252498448D 03	0.215250615844D 03	0.168260392789D-02
0.218000000000D 03	0.209464193246D 03	0.209463097141D 03	0.109610524396D-02
0.219000000000D 03	0.203852741559D 03	0.203852741559D 03	0.248689957516D-13
0.220000000000D 03	0.198412107074D 03	0.198417301338D 03	-0.519426438754D-02
0.221000000000D 03	0.193136480719D 03	0.193156793127D 03	-0.203124082286D-01
0.222000000000D 03	0.188020271319D 03	0.188064945792D 03	-0.446744726403D-01
0.223000000000D 03	0.183058096672D 03	0.183135719948D 03	-0.776232757051D-01
0.229000000000D 03	0.156242633526D 03	0.156564335714D 03	-0.421702188640D 00
0.233000000000D 03	0.141611890377D 03	0.141508571597D 03	0.331878055081D-02
0.237000000000D 03	0.128303946660D 03	0.128303946660D 03	0.284217094304D-13
0.245000000000D 03	0.105646314722D 03	0.105642771638D 03	0.554308315159D-02
0.250000000000D 03	0.937586310738D 02	0.937487761412D 02	0.985493260362D-02
0.270000000000D 03	0.590301268805D 02	0.590233812922D 02	0.674558833808D-02
0.279000000000D 03	0.482902323517D 02	0.482397020943D 02	0.530257381655D-03
0.285000000000D 03	0.423415114719D 02	0.423456469834D 02	-0.413552152309D-02
0.299000000000D 03	0.313821645875D 02	0.314306093484D 02	-0.484447609329D-01
0.342000000000D 03	0.134720611316D 02	0.134712759807D 02	0.785150904546D-03
0.410000000000D 03	0.398871539430D 01	0.408449712729D 01	-0.957817329940D-01
0.480000000000D 03	0.129181693981D 01	0.129159554315D 01	0.221396651137D-03
0.550000000000D 03	0.449473286944D 00	0.453450297264D 00	-0.397701031921D-02
0.650000000000D 03	0.112075750808D 00	0.112756896810D 00	-0.681146001936D-03

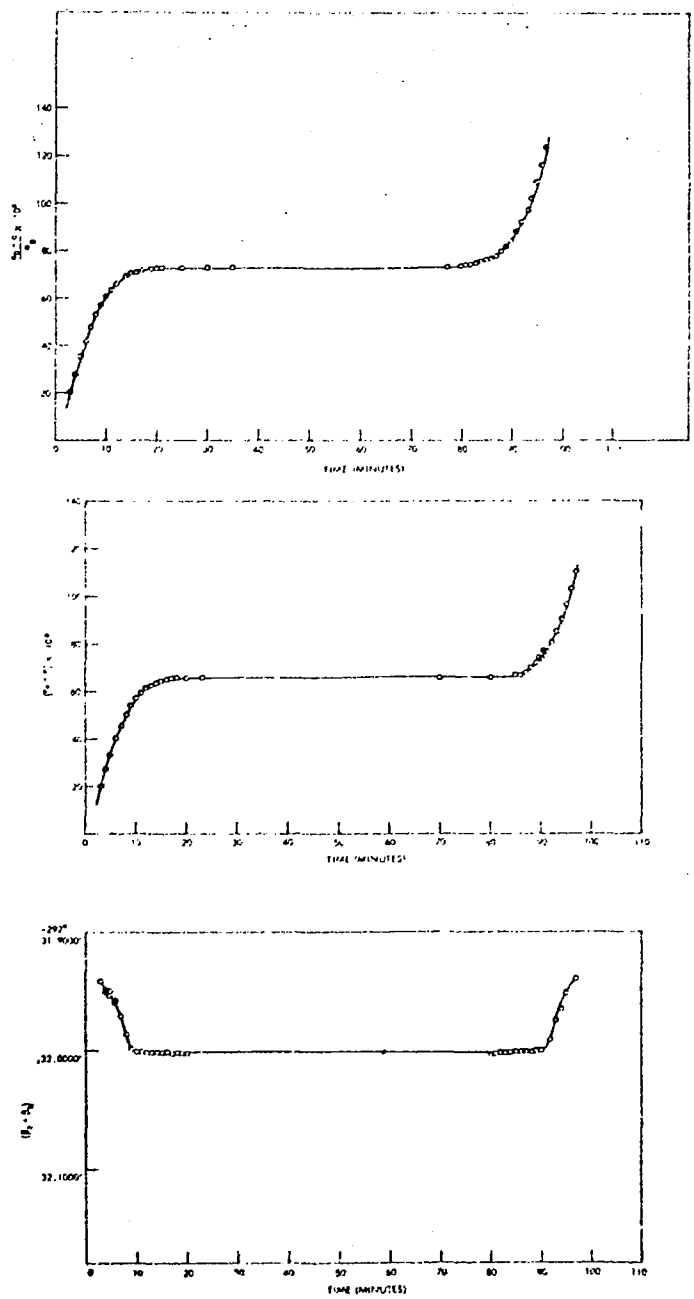

Figure 1. Variation of a, e, and $(\beta_2 + \beta_3)$ for San Marco-2

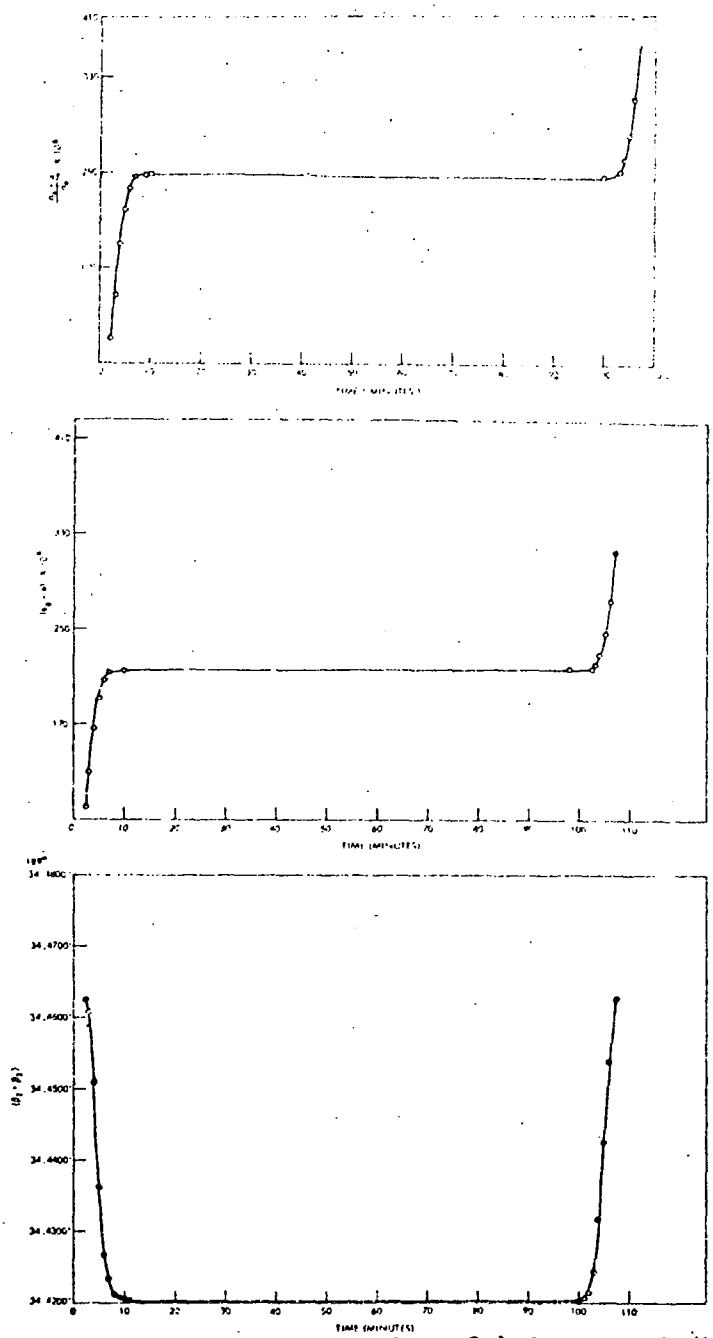

Figure 2. Variation of a, e, and $(\beta_2 + \beta_3)$ for Cannonball

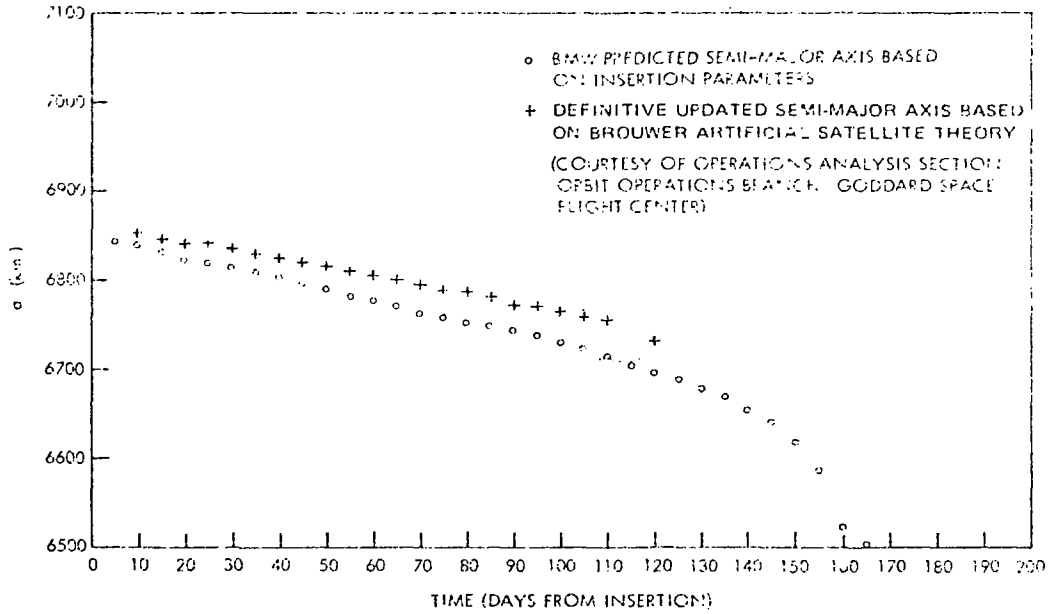

Figure 3. Variation of Semi-Major Axis for San Marco-2

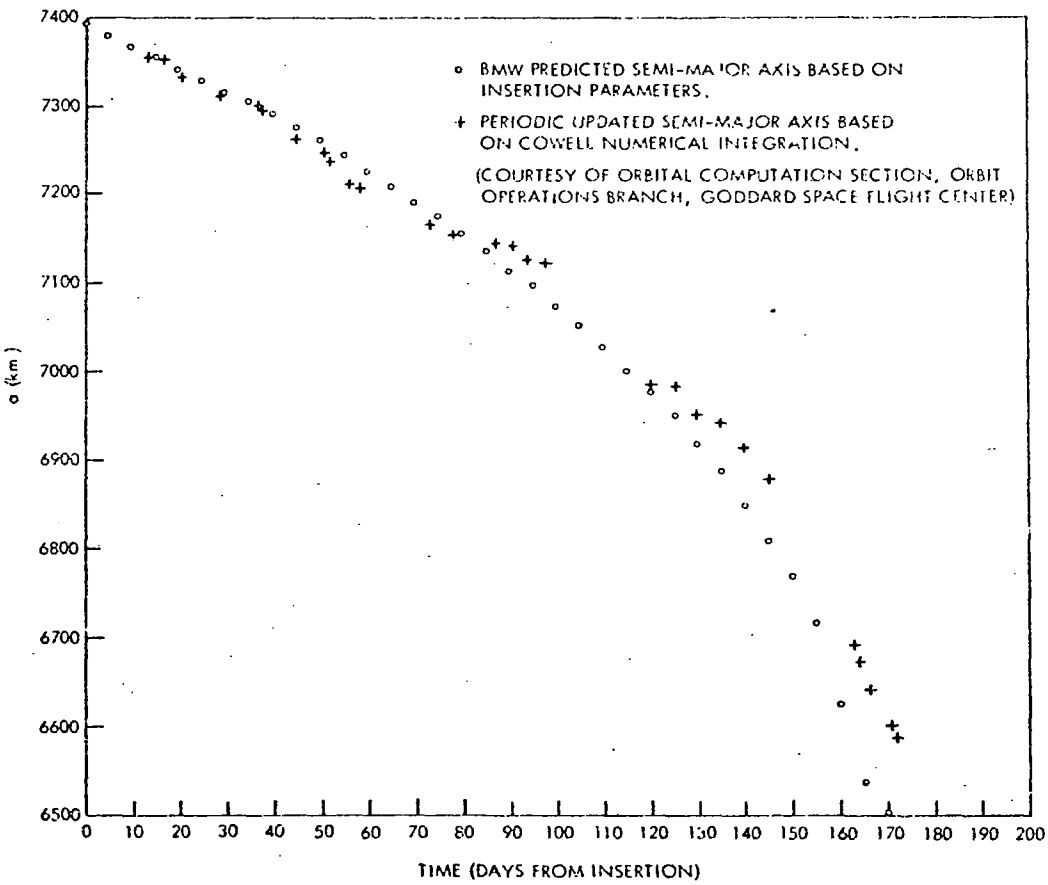

Figure 4. Variation of Semi-Major Axis for Cannonball

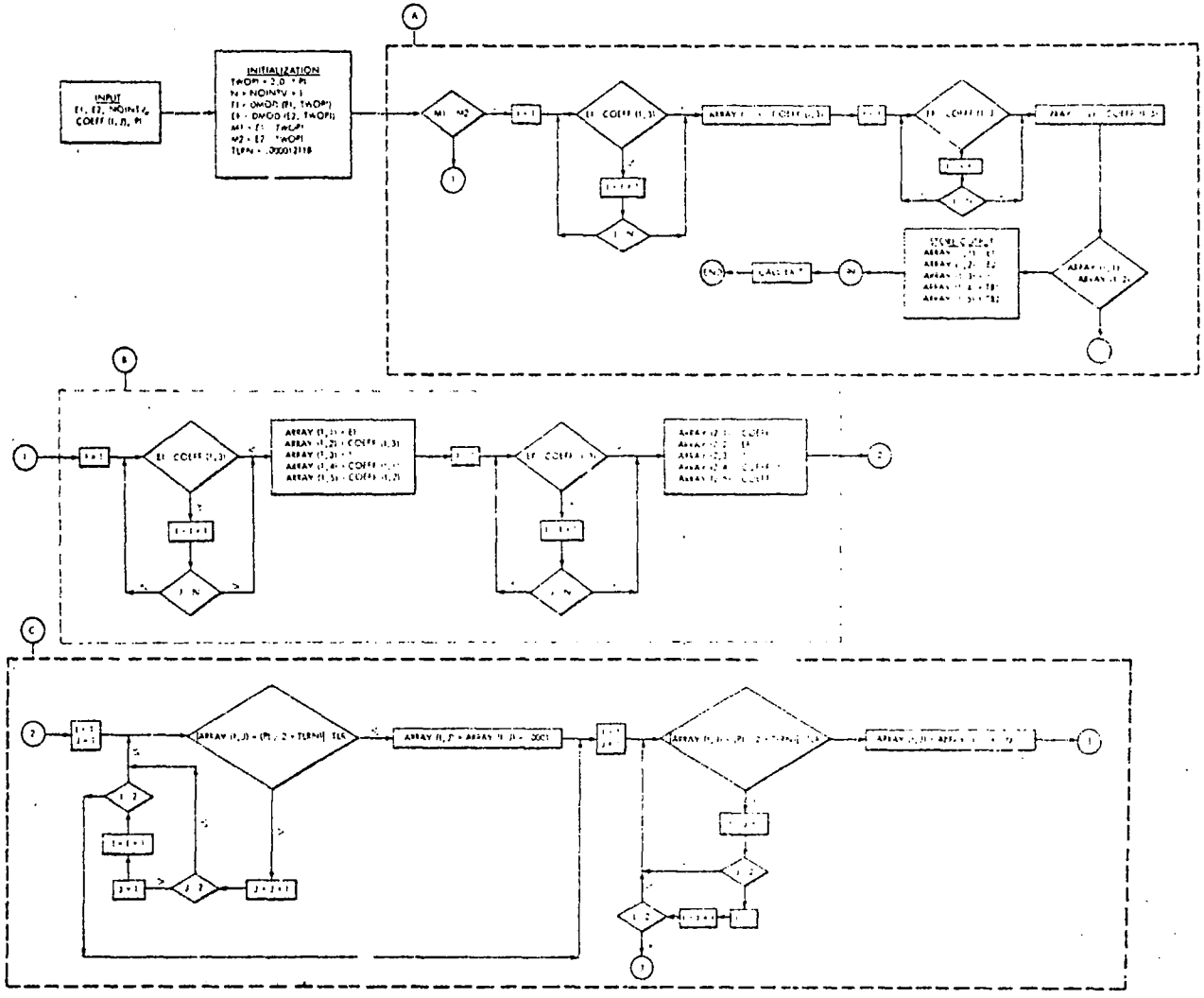

Figure A-1

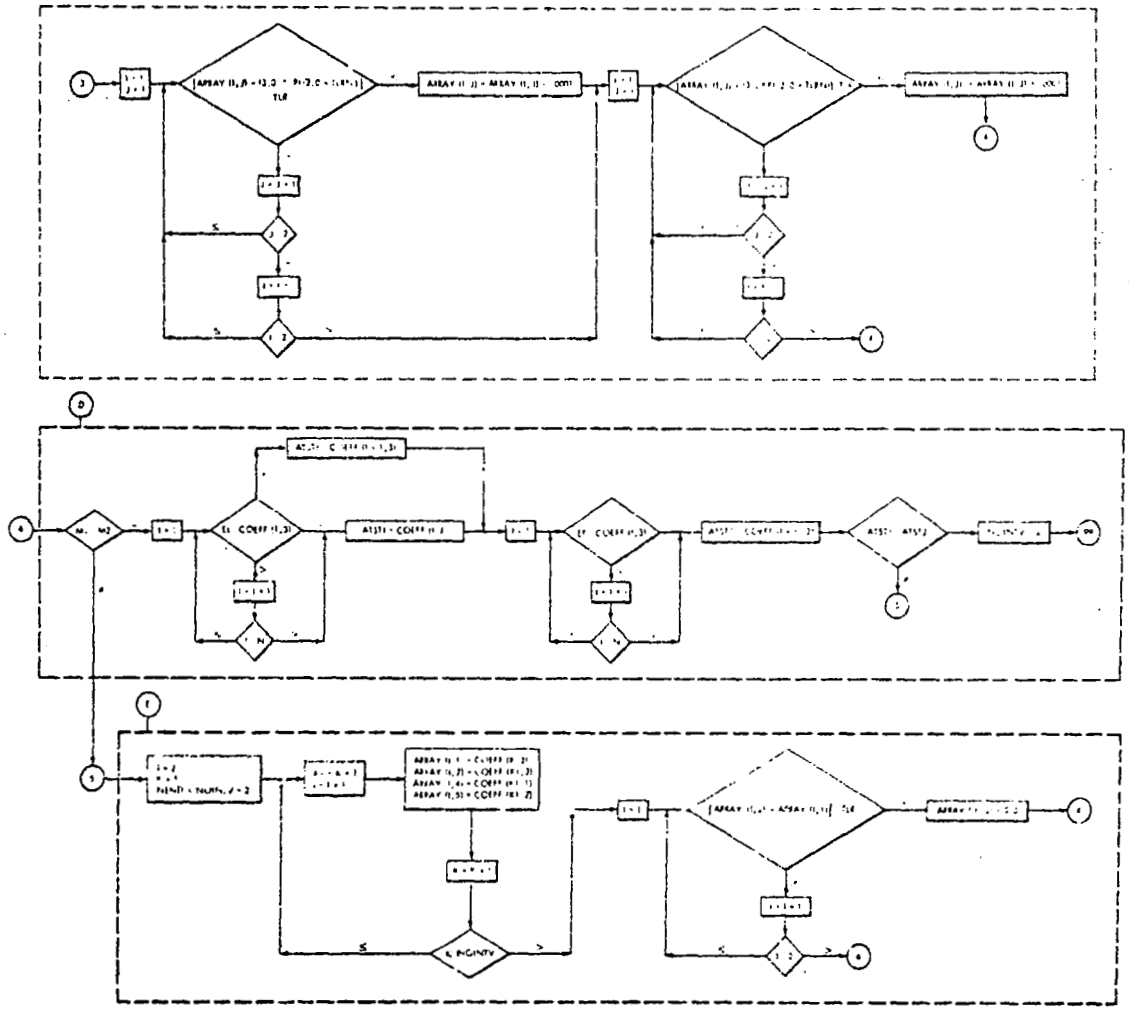

Figure A-1 (continued)

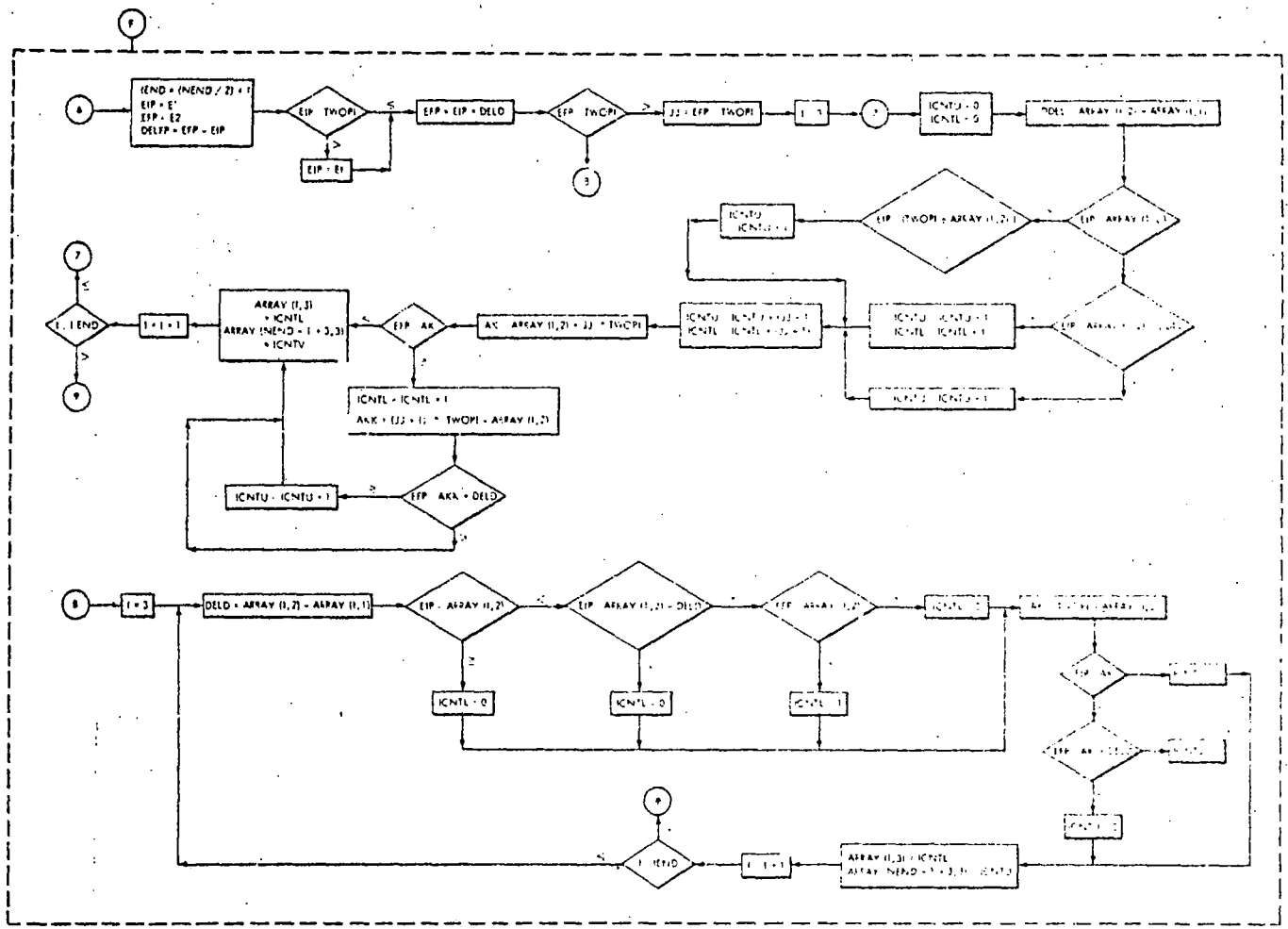

Figure A-1 (continued)

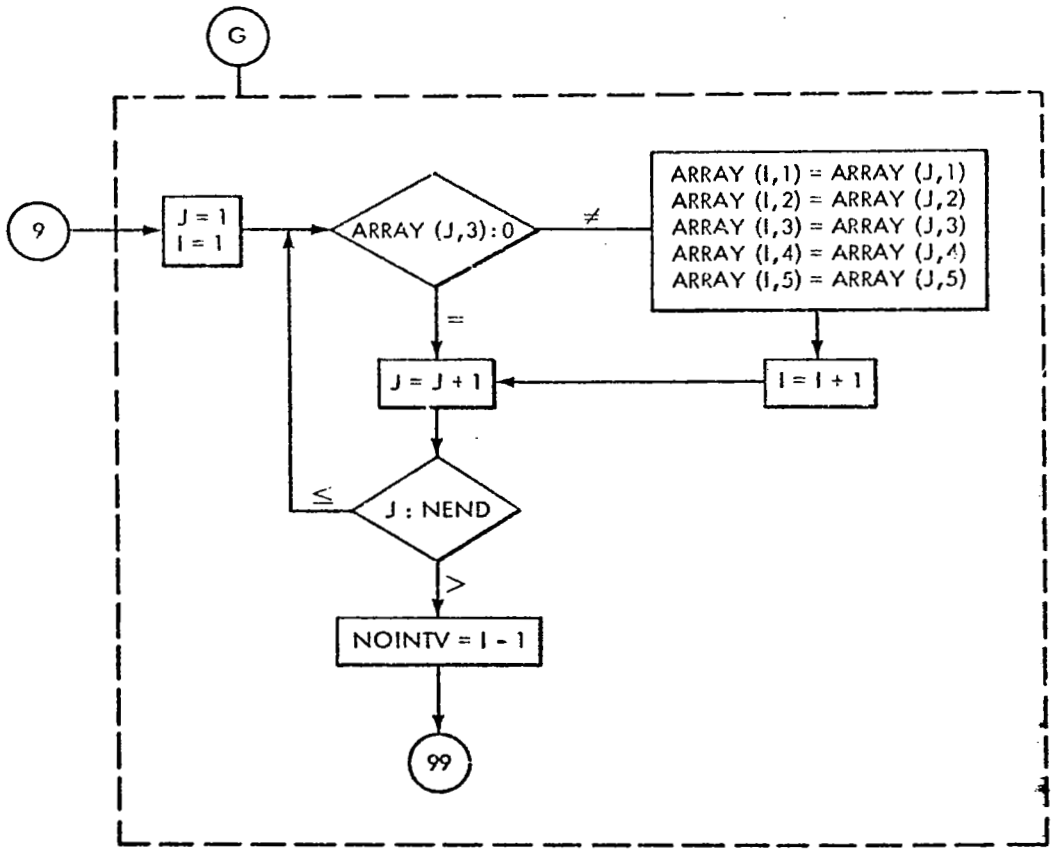

Figure A-1 (continued)

APPENDIX

DEVELOPMENT OF VARIATIONAL EQUATION CONSTANTS

For k = 1, 2, . . ., 6; the general expression for the change in the Vinti orbital elements due to atmospheric drag between the arbitrary limits E_1^*, E_2^* is given by:

$$\begin{aligned}
\Delta q_k = & \sum_{j=0}^{n-1} m_{j+1} \int_{x_j}^{x_{j+1}} \{ t_{j+1} \exp [d_{j+1} E] \} \, dG_k(E) \\
& + \sum_{j=0}^{n-1} m_{2n-j} \int_{2\pi - x_{j+1}}^{2\pi - x_j} \{ t'_{2n-j} \exp [d'_{2n-j} E] \} \, dG_k(E) \\
& + \int_{x_\xi}^{E_2^* \bmod 2\pi} t_\xi^* \exp [d_\xi^* E] \, dG_k(E) \\
& + \int_{E_1^* \bmod 2\pi}^{x_\eta} t_\eta^* \exp [d_\eta^* E] \, dG_k(E)
\end{aligned} \tag{A-1}$$

Without loss of generality, assume that the fitting process is performed over the interval $[0, \pi]$ i.e.

$$0 = x_0 < x_1 < x_2 < \cdots < x_{n-1} < x_n = \pi,$$

the coefficients t_ℓ are expressed by

$$t_\ell = c_\ell [1 + b(L, U) x^2 (\cos E_L - \cos E)^2] \quad (\ell = 1, 2 \cdots n) \tag{A-2}$$

where c_ℓ is a previously defined fitted parameter in the interval $I_\ell (x_{\ell-1}, x_\ell)$, $\ell = 1, 2, \ldots n$; $x = ae$, and $b(L, U)$ is derived by (II-14). From symmetry considerations define

$$x_{2n-\ell} = 2\pi - x_\ell \tag{A-3}$$

$$I_{2n-\ell+1} = (2\pi - x_\ell, 2\pi - x_{\ell-1}) \tag{A-4}$$

$$t'_{2n-\ell+1} = c_\ell \exp(2\pi d_\ell) [1 + b(L, U) x^2 (\cos E_L - \cos E)^2] \quad \ell = 1, 2, \ldots n \tag{A-5}$$

$$d'_{2n-\ell+1} = - d_\ell \tag{A-6}$$

$$c'_{2n-\ell+1} = c_\ell \tag{A-7}$$

where d_ℓ is the other previously defined, subinterval dependent, fitted parameter.

The remainder of this appendix shows the procedure utilized to derive the values of the non negative integer multiplicity factors m_ℓ, $m_{n+\ell}$ $\ell = 1, 2, \ldots n$; the value ξ, an integer between 0, 2n - 2; the value of η, an integer between 1, 2n - 1; and (t^*_ξ, t^*_η) which may be (t_ξ, t_η), (t'_ξ, t_η), (t_ξ, t'_η), or (t'_ξ, t'_η) depending upon whether E_1^* mod 2π and E_2^* mod 2π are less than or equal to or greater than π, for arbitrary E_1^*, E_2^* and for different modes of operation of the orbit

program. Prior to defining this procedure, consider the following definitions concerning (A) modes of operation of the Vinti orbit generator program, (B) integration intervals of the variational equations, and (C) Fortran variable definitions.

(A) Mode I

The Vinti orbit generator program is operating in mode I when the time span of the variational equation integration [or implicitly, the integration interval (E_1^*, E_2^*)] is sufficiently small so that there is not a complete fitting subinterval imbedded between the integration limits. Mode I will be the dominant mode for definitive ephemerides or an ephemeris computed to support a differential correction.

Mode II

The Vinti orbit generator is operating in mode II when the time span of variational integration has one or more imbedded fitting subintervals between the limits of variational equation integration. This mode will be utilized in lifetime studies when large intervals of integration will be performed. Note that mode II implies the assumption of a valid fit (or $\dot{x} \approx$ constant) over large periods of time than does mode I where new fits will be performed as frequently as is required.

(B) Class I Interval

A class I interval is an interval such that both boundary points are adjacent grid points of the mesh $x_0, x_1, \ldots, x_n$.

Class II Interval

A class II interval is an interval such that one boundary point of the interval is a point x_j of the mesh $x_0, x_1, \ldots, x_n$ while the other boundary point is a non mesh point between

$$x_j \text{ and } x_{j+1}.$$

(C) Fortran Variable Definitions

Fortran Variables	Mathematical Description
E1	E_1^*
E2	E_2^*
NOINTV	$2n$
COEFF (I, J) J = 1, I = 2, NOINTV/2 + 1	c_1 to c_n
COEFF (I, J) J = 1, I = NOINTV/2 + 2, NOINTV + 1	c_{n+1} to c_{2n}
J = 2, I = 2, NOINTV/2 + 1	d_1 to d_n
J = 2, I = NOINTV/2 + 2, NOINTV + 1	d'_{n+1} to d'_{2n}
J = 3 {I = 1, NOINTV + 1	$x_0, x_1, \cdots x_{2n}$

ARRAY (I, J)

$$I = 1 \begin{cases} J = 1 & E_1^* \bmod 2\pi \\ J = 2 & x_\eta \\ J = 3 & 0 \text{ or } 1 \\ J = 4 & t^*_\eta \\ J = 5 & d^*_\eta \end{cases}$$

$$I = 2 \begin{cases} J = 1 & x_\xi \\ J = 2 & E_2^* \bmod 2\pi \\ J = 3 & 0 \text{ or } 1 \\ J = 4 & t^*_\xi \\ J = 5 & d^*_\xi \end{cases}$$

$$I = 3, \text{NOINTV} + 2 \begin{cases} J = 1 & x_0, x_1, \cdots, x_{2n-1} \\ J = 2 & x_1, x_2, \cdots, x_{2n} \end{cases}$$

$$I = 3, \frac{\text{NOINTV}}{2} + 1 \begin{cases} J = 3 & m_\ell \\ J = 4 & c_\ell \\ J = 5 & d_\ell \end{cases}$$

$$I = \frac{\text{NOINTV}}{2} + 2, \text{NOINTV} + 2 \begin{cases} J = 3 & m_{n+\ell} \\ J = 4 & c'_{n+\ell} \\ J = 5 & d'_{n+\ell} \end{cases}$$

The following describes the subtasks associated with defining the full set of integration parameters in (A-1). The detailed logic is presented in the flowchart given in Figure A-1.

Ⓐ This algorithm will test whether E_1^* and E_2^* are within the same subinterval, will store the proper interval of integration and associated constants into ARRAY, and exit. This simplified logic is most useful in Mode I orbit generations.

Ⓑ This algorithm defines the Class II intervals associated with the arbitrary limits E_1^*, E_2^*, (i.e. $[x_\xi, E_2^* \bmod 2\pi]$ and $[E_1^* \bmod 2\pi, x_\eta]$) and stores them and the associated constants into ARRAY.

Ⓒ This algorithm checks to see if any of the Class II intervals are near $\pi/2$ or $3\pi/2$ in order to avoid underflow difficulties during evaluation of the integrals.

Ⓓ To assist the task of deleting unnecessary computations in Mode I generations, this algorithm establishes the necessary intervals and associated constants when E_1^* and E_2^* are in adjacent subintervals and in the same multiple of 2π.

Ⓔ This logic stores the entire set of Class I subintervals and associated constants into ARRAY and checks the Class II subintervals for negligible length. If such a Class II interval is found, it is eliminated from consideration. An arbitrary interval length of 1×10^{-7} is the criterion presently used.

Ⓕ This algorithm defines m_{ℓ}, $m_{n+\ell}$. It is predominantly used in Mode II orbit generations.

Ⓖ This algorithm redefines ARRAY to eliminate Class I intervals with a multiplicity factor of zero and Class II intervals whose multiplicity factor has been reset from one to zero by Ⓔ when its length is negligible.

END

DATE

FILMED

SEP 26 1973